

An application of Audiomagnetotelluric prospecting method to determine the dip of the sedimentary-metamorphic contact

Njingti-Nfor¹, Tadjou J.M.² and Nouayou R³

¹Department of Physics, Advanced Teachers' Training College, University of Yaounde I; Cameroon

²National Institute of Cartography, Scientific and Technical Research, Cameroon;

³Department of Physics, Faculty of Science, University of Yaoundé I, Cameroon

Abstract

From the geometric mean values of apparent resistivity, iso-resistivity contour maps were drawn using audiomagnetotellurics data collected along two profiles traversing the metamorphic and sedimentary formations. On these maps, resistivity discontinuity observed along the contour lines indicated the existence in this area of a contact between two blocks of different lithologies. By drawing tangents along a specific contour line ($20 \Omega\text{m}$) which is considered as reference separating the two formations, the dips of down dropping under each station were calculated. The values of dip in the sedimentary formation, which have maximum values of 10° at a depth of 1400 m and 17° at a depth of 800 m,

were suggestive of a pronounced westward lateral spread. The values of dip at contact between the sedimentary and the metamorphic formations at various depths beginning from the surface varied from 58° to 73° for one profile and from 21° to 60° for another profile, showing that the contact is abrupt and deep-seated with little lateral spread at depth. The results of our study have confirmed the fact that the contact between the metamorphic and sedimentary formations can be recognised through a sharp and distinct resistivity contrast along a given profile.

Keywords: Audiomagnetotellurics, dip, discontinuity, contact, iso-resistivity, deep

I. INTRODUCTION

The onshore Douala sedimentary basin situated at the edge of the Gulf of Guinea extends from latitudes $3^\circ 15' \text{ N}$ to $4^\circ 30' \text{ N}$. This basin is about 60 km long and covers an estimated surface area of 7000 km^2 . It is bordered to the East by the Precambrian rocks of the Congo Craton. To the North and North-west, it is separated from the Rio-del Rey basin by the Cameroon Volcanic Line. To the South, it tapers towards Kribi and outcrops in the Campo area.

The basin marks the transition between the Niger Delta basin to the Southwest and the Gabon basin to the Southeast. Part of the area consists of estuaries of the Wouri, Sanaga, the Dibamba and the Moungo rivers. The basin itself is low-lying with an average altitude of about 100 m above sea level, flat and swampy around the estuaries and is covered with coastal sands and generally blanketed with mangrove forest, characteristic of sedimentary basins (Figure 1).

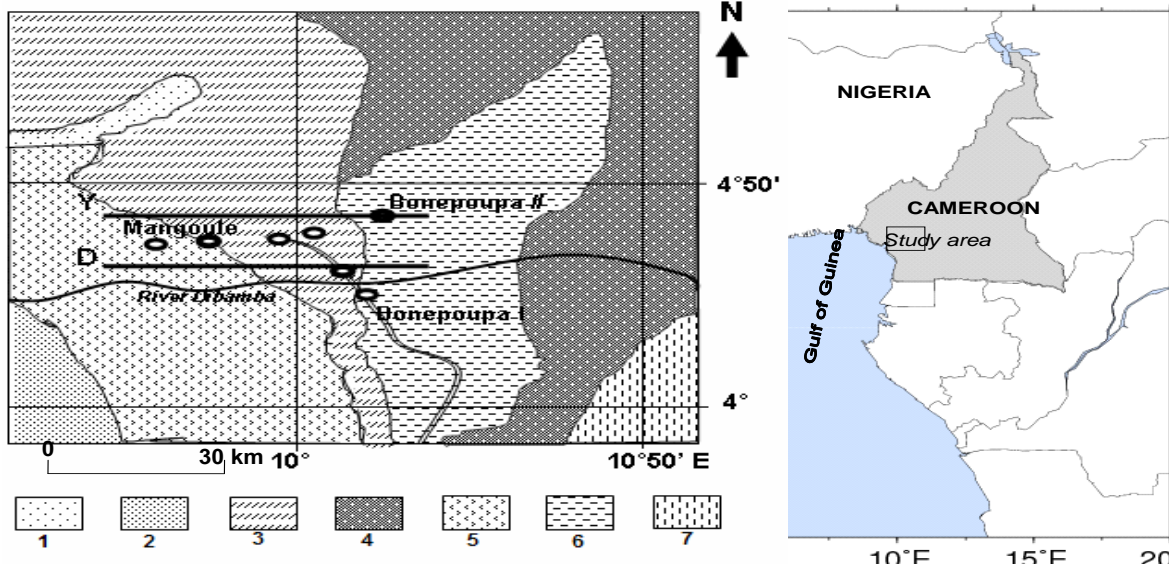


Figure 1: A geologic map of the eastern edge of the Douala basin showing the location of magnetotelluric stations and profiles.

- 1: Alluvium, lacustrine clay; 2: Shale, clay, greywacke (Paleocene); 3: Basal sandstone facies (Albian-Senonian);
4: Embrechite gneiss, Amphibolites; 5: Quartzite; 6: Muscovite gneiss, sillimanite and hypersthenes with quartz composition; 7: Granitised gneiss, undifferentiated gneiss and migmatite; 8: Magnetotelluric sounding station

The basins of the African continent date from the Mesozoic and subsequently have been filled with continental lacustrine evaporitic and normal marine sediments. Most of the coasts south of the Equator either have low cliffs of Precambrian igneous and metamorphic rocks where the basement reaches the coast or of Mesozoic and Cenozoic strata, where coastal basins are being eroded [1]. The origin of the Douala basin is directly linked to the opening of the South Atlantic during the Cretaceous [2].

The sedimentary column of the Douala basin has a Precambrian basement overlain by Mesozoic and Cenozoic sediments which are characterised by coarse detrital deposits of variable thickness known as "basal sandstones" [2]. The basal sandstones are essentially composed of arkosic sandstones and conglomerates. Lying above these coarse grained sedimentary rocks are marine shale, sandstones and limestone of Albian-Santonian age ([3], [4]). To the West of the basin is found mostly marshes and to the East are Quaternary alluvial deposits [5]. The sand deposits are generally coarse with colours ranging from brick red to chocolate brown, arranged in slate (platform) or leaflets and cemented with goethite and sometimes

haematite. Minerals found in the sand apart from quartz and clay are ilmenite, magnetite, muscovite, hornblende, hypersthenes, zircon, garnet, kyanite and sillimanite probably drained into the plains of the basin by the Moung, Dibamba, and Wouri rivers from western Cameroon and by the Sanaga river from Adamawa region.

The zone under study is around the Dibamba river and forms part of the Louangahe series which is one of the four stratigraphic series that outcrop at the edge of the Cameroon Atlantic coast ([6], [7], [8], [9]). The series consists of coarse unconsolidated sandstones mixed with marls, calcareous and silty clay whose age is considered as Senonian [6]. This forms a facies, which is diachronous of the Aptian-Albian and Upper Senonian (in Campo and Moung) basin respectively. The important fact about the series is that it marks the sedimentary-crystalline (metamorphic) contact. Its thickness is estimated to be between 500 to 600 m [10] and was deposited in a piedmont type sedimentation, which seems to have been successively confined and opened into the sea in a chisel-like mechanism [11] and which was concurrently filled with sediments of the proto-gulf of Guinea [12].

II. METHODOLOGY

A. Geometric mean values of apparent resistivity

The instrument used to collect the audiagnetotelluric data is the ECA 540 AMT resistivity meter, which has a frequency range from 4.1 Hz to 2300 Hz giving a total number of twelve frequencies [13]. The audiagnetotelluric data collected give the fundamental information necessary for the analysis and interpretation. These data are never complete and may not generally be very exact due to inherent uncertainties brought about by natural and artificial errors. The natural uncertainties are associated to the erratic nature of the telluric currents caused by natural factors like cosmic radiations. While the artificial factors could be the presence of an electric grid line and road traffic in the vicinity of the prospecting [14]. Generally, these uncertainties are minimised in the field by taking a series of up to five values of apparent resistivity for each value of frequency and from a field curve, determining the line-of-best fit [15]. But these resistivity values equally depend on the presence of pore fluid and their salinity within the rocks, which are not constant as they too depend on both the season, the temperature, the pressure and the degree of compaction of the rocks [16]. These, thus introduce other uncertainties, which can

be important in sedimentary areas because of the high conductivity, but are generally minimal in metamorphic areas where rocks are highly resistive. Conventionally the methods used to analyse and interpret data included: plotting sounding curves, plotting resistivity profiles, drawing pseudo-sections, and drawing geoelectric sections for each of the principal directions [17]. However, [18] introduced new methods of analysis and interpretation of audiagnetotelluric data, which consist essentially of calculating geometric mean values of apparent resistivity and, using the data so obtained, to draw iso-resistivity contour maps. According to the same author, the geometric mean and not the arithmetic mean, is considered because intervening factors such as geologic time and texture, contact, temperature and pressure variations on allochthonous or autochthonous rocks, always have an influence from the surrounding rocks that makes the variation in resistivity from one rock type to the other continuous and not discrete. Thus this method supposes that for each frequency, and for the values of apparent resistivity got in the two principal

directions, the geometric mean value $\bar{\rho}_a$ can be calculated using the formula:

$$\bar{\rho}_a = \sqrt{\rho_t \rho_l} \quad (1)$$

where ρ_t is the transverse resistivity and ρ_l is the longitudinal resistivity. This gives sets of geometric mean values of apparent resistivity for each frequency that are used to draw iso-resistivity contour maps. It is from such iso-resistivity contour maps that the angles of dip at various points of contact between the sedimentary and metamorphic basement in the eastern

edge of the Douala sedimentary basin are determined in this work. The pseudo-depth of penetration The principle of the "skin-effect" according to which the depth of penetration of the telluric current decreases with an increase in frequency is used to determine the pseudo-depth of penetration. Therefore, from the geometric mean values of resistivity for each frequency, the depth of penetration in kilometres is calculated using the formula:

$$P = 0.503\sqrt{\rho_a/f} \quad (2)$$

where f is the applied frequency in Hz, P in km. From field observations, the depth of penetration in the Douala sedimentary zone is shallow (down to a maximum of about 4.2 km). This might be due to the fact that the AMT resistivity meter uses higher frequencies, which in turn means low penetration depths brought about by a rapid attenuation of the telluric current, due to the high conductivity of sedimentary rocks. The same situation is not obtained in the metamorphic zones, where the rocks are very resistive, and depths of about 50 km or more could be attained [17].

B. Dip of contact from iso-resistivity contour map

There are two ways by which the dip of a geologic structure can be calculated from the iso-resistivity contour map. The first way is by

C. Spatial distribution of stations

For each station, twelve series of measurements were made for the component of the electric field intensity, its mutually perpendicular component of magnetic field intensity and values of apparent resistivity in the two predetermined directions. These directions were determined using the method of rotation [17]. In the field, station-to-station spacing is determined with respect to the nature of the subsurface (which could be as a result of geological investigations already done in the area of research). In such a situation, stations are close together around suspected structural and/or resistivity discontinuities and more spaced out where there are little or less important disruptions. In the case of the present study, the choice of the area of study was based on the fact that it lies within the

following the lateral evolution of a given iso-resistivity contour line beginning from the station nearest to the contact or suspected discontinuity to stations furthest away from it. Using this contour line as the reference, the slope of the contact under each station along the profile can be calculated by drawing a tangent to the contour line at that point and looking for its gradient. The second way is by following the evolution with depth of the contact as we move from the contour line nearest to the surface to the one right in the subsurface. This is done for the station(s) closest to the contact or suspected discontinuity chosen as reference(s). Figure 2 is an illustration of how the calculation can be done.

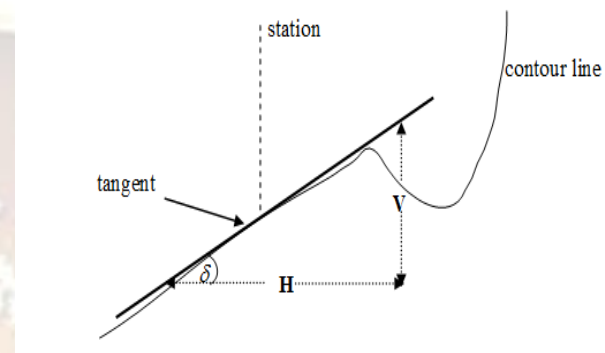


Figure 2: Method of the calculation of dip source using iso-resistivity contour

he dip is then calculated using the equation [16].

$$\tan(\delta) = \left(\frac{V}{H} \right) \quad (3)$$

where V is the vertical separation of two points on the contour line and H is the horizontal separation measured in the same units as V. The dip direction at any point will be parallel to the tangent or the contour line in case the two coincide.

zone of sedimentary-metamorphic basement contact, where [10] reported the presence of a tectonic fault. However, three factors influenced the choice of the station-to-station spacing. The stations were implanted in a zone where there is easy accessibility because of the mangrove nature of the vegetation. They were also implanted far from the electric grid whose current can influence the telluric current values ([14], [19]). The unelectrified part of the highways was considered. Thirdly, stations were chosen such that they were close together near suspected discontinuity and more spread out away from it. The principal directions of the measurements were chosen as N-S and E-W [17], the edge under consideration being in the region but oriented close to the N-S direction.

D. Presentation of profiles

In the analysis and interpretation of data, stations are projected along an axis so that they all lie on a straight line and thus constitute a profile. This is done in order to make maximum use of the information gathered from the field and also for easy analysis and interpretation. The projection is made in such a way that all the stations lie perpendicular to the line of structure (contact) to be determined. One of the stations (the most westerly located in this case) is chosen as base-station with respect to which the distances to all the other stations are determined. The work that was carried out in this zone was done for two profiles Y and D (Figure 1). Profile D extends from Bonepoupa I (close to river Dibamba) to Mangoule (on the road to Douala), covering a

distance of about 13 km but 9 km when projected. It comprises five stations D_1 , D_2 , D_3 , D_4 , and D_5 . Profile Y extends from Mangoule to Bonepoupa III (on the way to Yabassi), covering a total distance of 16 km but 8 km when projected. This equally comprises five stations Y_1 , Y_2 , Y_3 , Y_4 , and Y_5 , with Y_1 and Y_2 coinciding with D_5 and D_4 respectively. The average station-to-station spacing is about 1.5 km. In the analysis and interpretation, profile D is a projection from West to East of all the stations along the original profile Y, with D_5 as origin. Profile Y is a projection from West to East of all the stations along the original profile D, with Y_3 as origin. Thus the two profiles are parallel to each other.

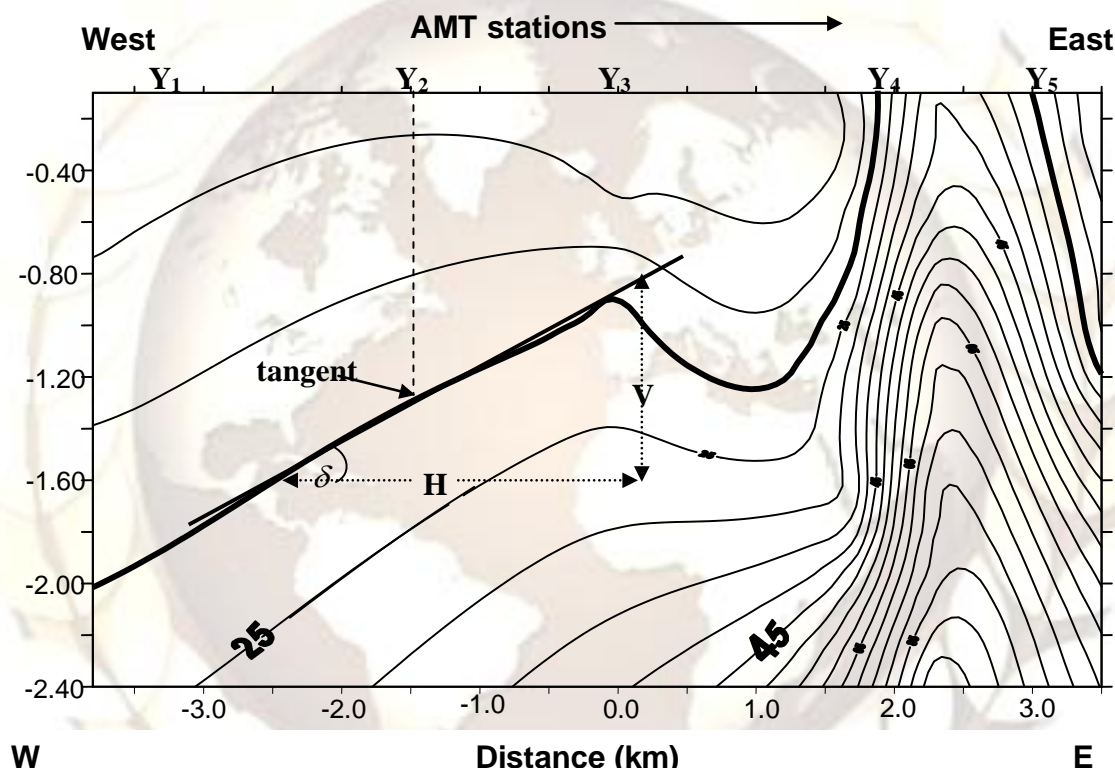


Figure 3: Iso-resistivity contour map of profile Y

E. Iso-resistivity contour maps

In a vertical plane with the lateral distance of other stations from the base-station along the horizontal axis, the pseudo-depth of penetration in the vertically downward directed axis, the geometric mean of the apparent resistivity values are plotted. When points of the same geometric mean apparent resistivity values are connected together, the line constitutes an iso-resistivity contour line [18]. Such lines drawn for all the geometric mean values in a profile give the iso-resistivity contour map. This indicates the variation of the geometric mean values of apparent resistivity with depth along a lateral direction perpendicular to the line of structure or direction of minimum resistivity. These contour maps provide a more effective and efficient

representation of the variation of apparent resistivity with depth for a vertical cross-section through a slice of Earth. They illustrate the shape of structure(s) within the sub-surface. If the sub-surface is homogeneous and has uniformly varying apparent resistivity values, the contours are horizontal and parallel, uniformly spaced and unfolded. Abrupt changes in the values of apparent resistivity are indicated on the contour maps by curved contours. These might represent folds, faults, contacts or intrusions. The contour intervals are determined from the range of apparent resistivity values. In the present study, the prospecting was done in a sedimentary region, where the apparent resistivity values are in tens or hundreds of ohm-metres and the

contour intervals have been chosen based on this

variation.

III. PRESENTATION OF RESULTS

Iso-resistivity contour maps

The Audiomagnetotelluric data used in this work enabled authors to locate precisely a metamorphic basement-sedimentary contact in this zone. But they were not able to give an estimate of the dip of the contact around the area of study. The iso-resistivity

maps drawn from the geometric mean values of apparent resistivity for the two profiles Y and D, which are both oriented from west to east are presented in Figures 3 and 4 respectively.

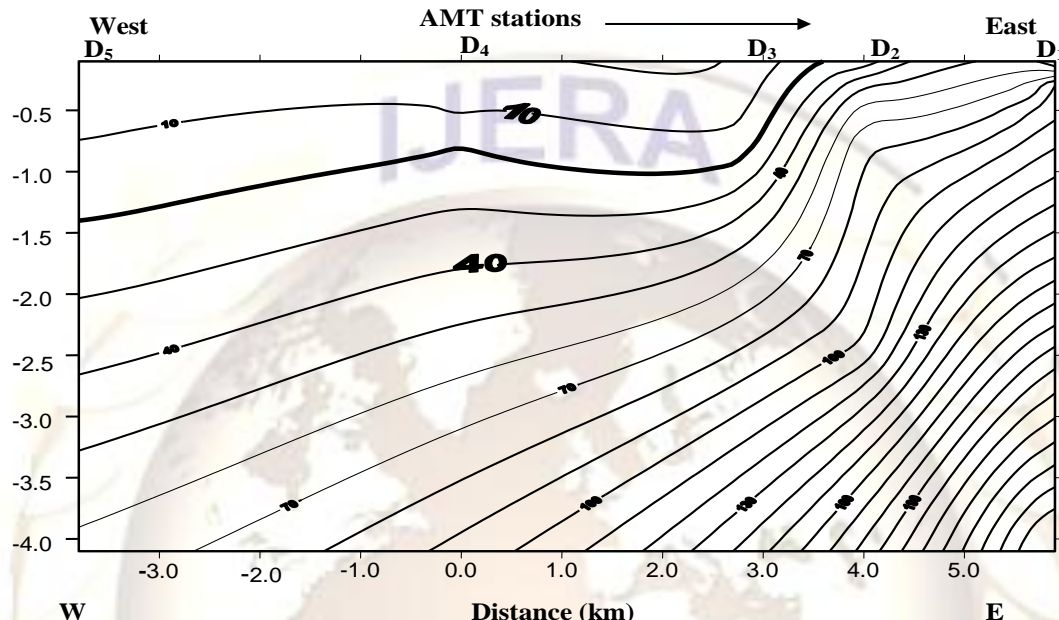


Figure 4: Iso-resistivity contour map of profile D

Profile Y has a total length of about 8.0 km and a maximum pseudo-depth of penetration of about 2.4 km. Profile D has a total length of about 9.0 km and a maximum pseudo-depth of penetration of about 4.2 km. On each profile, the most westerly located portion is the sedimentary formation while the metamorphic formation is found close to the Far-East. The iso-resistivity contour lines in the sedimentary area are sparsely distributed, but are

very closely packed in the metamorphic area with the lines almost vertically plunging. What is more remarkable for both profiles is that the contours on the metamorphic portions are highly distinct and highly concentrated. [15] equally identified the two distinct blocks in their work. Applying equation (3) on figures 3 and 4 the values of dip are calculated and the results are as presented in tables 1 to 5.

IV. INTERPRETATION AND DISCUSSION OF RESULTS

A. Profile Y (Figure 3)

The values of the dip along the $20\Omega\text{m}$ contour line under stations Y_1 , Y_2 , and Y_3 , as presented in Table 1, are very low and apparently constant. Starting from a depth of 1900 m below station Y_1 , the contour rises gradually to a depth of 900 m under station Y_3 that is at the crest of an anticlinorium, which is not visible at the surface. This is shown by a change of angle of dip from a positive value of 16° to a negative value of -22° as we move along the contour line from west to east. At Y_4 , the dip is extremely high with a positive value of 73° , which changes to a negative but still high value of -63° at Y_5 . These high values

indicate a discontinuity along the contour line with a flat top between Y_4 and Y_5 . The change in the sign of dip indicates the presence of an anticline between Y_4 and Y_5 , whose crest has probably been eroded with time leading to a flat top of about 1100 m of lateral distance. As we move down into the subsurface below station Y_4 and at contour intervals of $10\Omega\text{m}$, the calculated angles of dip at different depths are as presented in Table 2. The $20\Omega\text{m}$ contour line has a distinguishingly high dip of 73° at surface level.

Table 1: Dip at contact along west-east orientation of the $20 \Omega m$ contour line for profile Y

Station	Y ₁	Y ₂	Y ₃	Y ₄	Y ₅
Depth in km	1.9	2.1	0.9	0.0	0.0
Vertical separation (V)	0.8	0.8	0.8	0.8	1.6
Horizontal separation (H) in km	2.6	2.75	2.75	-2.0	0.5
Value of dip	17°	16°	16°	-22°	73°
					-63°

The other values, which are equally high, are constant at 58° and occur at various depths ranging from 700 m to 2300 m below the surface. The high values show that there is an abrupt and almost sub-vertical discontinuity under this station. The constant values indicate that near the discontinuity, contour lines are parallel and have very little lateral spread with depth. To the far-east of profile Y, below station Y₅, the values of dip at contour

intervals of 10 Ωm and at various depths are as presented in Table 3. All the values are negative and have magnitudes of about 60° . The negative values indicate that the contour lines are plunging downward from west to east. The high values show that there is an abrupt discontinuity around this station, which has constant magnitude of dip and therefore should show very little lateral spread with depth.

Table 2 :Dip at contact on the different contour lines under station Y₄ line for profile Y

Contour lines in (Ωm)	20	30	40	50	60	70
Depth in km	0.0	0.7	1.0	1.7	2.0	2.3
Vertical separation (V)	1.6	0.8	0.8	0.8	1.2	1.2
Horizontal separation (H) in km	0.5	0.5	0.5	.5	0.75	0.75
Value of dip	73°	58°	58°	58°	58°	58°

Table 3: Dip at contact on the different contour lines under station Y₅ line for profile Y

Contour lines in (Ωm)	30	40	50	60	70	80
Depth km	0.3	0.6	1.1	1.4	1.6	2.1
Vertical separation (V)	1.2	1.2	0.8	0.8	1.2	1.2
Horizontal separation (H) in km	-0.6	-0.7	-0.5	-0.5	-0.75	-0.75
Value of dip	-63°	-60°	-60°	-60°	-60°	-60°

B. Profile D (Figure 4)

The values of the dip along the $20\Omega m$ contour line under stations D₅, D₄, D₃, D₂ and D₁ are presented in Table 4. The values of dip vary as we move along the contour line from west to east. Under station D₅, at a depth of 1400 m, the value of 10° is low and positive. Under station D₄, the contour line is at 800 m and the value of dip is -11° , which is equally low

but negative, indicative of a low amplitude anticline between D₅ and D₄. Under station D₃ at a depth of 1200 m, the value of dip is 31° . This value is considered high showing that the station is at the edge of a discontinuity in the form of an anticline whose crest is occupied by stations D₂, and D₁, which both have a dip of 0° with the surface.

Table 4: Dip at contact along west-east orientation of the $20 (\Omega m)$ contour line for profile D

Station	D ₅	D ₄	D ₃	D ₂	D ₁
Depth in km	1.4	0.8	1.2	0.0	0.0
Vertical separation (V)	0.9	1.0	1.5	0.0	0.0
Horizontal separation (H) in km	5.3	-5.0	5.8	5.8	8.0
Value of dip	10°	-11°	31°	0°	0°

As we move down into the subsurface from a depth of 200 m to 3250 m below station D₂ and at contour intervals of $20\Omega m$, the calculated angles of dip are as presented in Table 5. From 200 m on contour $40 \Omega m$ to 800 m on contour $80 \Omega m$, the value of dip can be considered low varying from 21° to 24° . From a depth of 1750 m to 3250 m, the values of dip

become very high and constant at about 60° . The high values show the presence of an abrupt and sub-vertical discontinuity. The constant values indicate that contour lines are parallel and the discontinuity is highly concentrated having a gradual lateral spread with depth.

Table 5: Dip at contact on the different contour lines under station D₂ line for profile D

Contour lines in (Ωm)	40	60	80	100	120	140
Depth km	0.2	0.6	0.8	1.75	2.9	3.25
Vertical separation (V)	1.3	1.3	0.9	2.0	1.3	1.3
Horizontal separation (H) in km	3.3	3.3	2.0	1.0	0.75	0.75
Value of dip	21°	21°	24°	63°	60°	60°

V. CONCLUSION

Using pseudo-sections of transverse resistivity, the audiagnetotelluric method enabled us to locate the contact between the sedimentary-metamorphic basement formations thanks to the sharp resistivity contrast. The method of drawing iso-resistivity contour maps from geometric mean values used here has enabled us to confirm this result. From the iso-resistivity contour maps, we have been able to successfully calculate the dip at various positions and depths under each profile. Our results show that the values of dip under stations Y_1 , Y_2 , D_5 , and D_4 are low and apparently constant for each profile, suggestive of a greater westward lateral spread, which goes beyond the limit considered in this work, and should correspond to the sedimentary formation. It also shows that at contact between the sedimentary and the metamorphic formations, the dip is very steep with angles varying from 58° to 73°. For profile Y these angles of dip maintain nearly constant values of 58° with depth under station Y_4 that is to the west and of -60° under station Y_5 to east of the contact between the

sedimentary and the metamorphic formations. The metamorphic formation can therefore be observed on the surface between stations Y_4 and Y_5 with a lateral distance of about 1 km. On the other hand, for profile D the contact between the two formations is more pronounced only to the west of station D_2 with angles of dip increasing with depth from 0° at the surface to a very high and constant value of 60° at depth. The metamorphic formation can be observed at the surface to the east of D_3 . The values of dip got in this study are quite different from those got by earlier study which corresponds to 3%, that is only 2° for the top most sedimentary layer and vary between 12 and 13% that corresponds to about 7° between either stations D_4 and D_3 or Y_2 and Y_3 . Considering that the conclusions were drawn for transverse pseudo-section of resistivity we suspect that different values would have been got if the longitudinal pseudo-section was used and therefore conclude that the method used in the present study is much more revealing

REFERENCES

- [1]. **Adediran, S. A. and Adegoke, O. S. (1987).** Evolution of the sedimentary basins of the Gulf of Guinea, in G. Matheis and H. Schandlmeier (eds) Current research in sciences. Balkema Rotterdam p. 283-286.
- [2]. **Baptupe, M. (1996).** Aspect of the stratigraphic evolution of the Douala basin, Cameroon (abstract), in S. Jardiné, I. Deklasz and J. P. Debenay eds. Geologie d'Atlantique Sud: Elf Aquitaine edition memoir 16, p. 694.
- [3]. **Belmonte, Y. C. (1996).** Stratigraphie du basins sedimentaire du Cameroun, in J. E. Van Hinte (ed.): Proceedings of the second West African Micopaleontological colloquim, Ibadan. P. 7-24.
- [4]. **Emery K. O. (1975).** Continental Margin of Western African Angola to Serra Leone. Am. Assoc. Petrol. Geol. Bull. Vol. 59, No. 12, 2209-2265.
- [5]. **Hausknecht J. J. (1966).** Note sur l'étude photogeologique de la bordure du basin sedimentaire du Cameroun entre 3° et 4° N. Entreprise de recherches et activités pétrolières. Département Géologique Central.
- [6]. **De Vries (1936).** Mission de recherché des hydrocarbures du Cameroun. Effectuée en 1935-1936. Rapport Général, Service des mines du Cameroun. 72p.
- [7]. **Njike, N. P. R. (1984).** Contribution a l'étude géologique, stratigraphique et structurale de la bordure du basin atlantique au Cameroun. These Doc. 3^{eme} Cycle, Univ. Yaounde.
- [8]. **Njike, N. P. R. and Belinga, S. M., (1987).** Le Diachronisme du grès de base, le Paléoenvironnement et le rôle de l'ouverture de l'Atlantique Sud. Ann. Fac. Sci. Terre IV, No. 3-4, 103-119.
- [9]. **Njingti-Nfor Manguelle-Dicoum E., Tabod C. Tadjou J. M. (2001).** Application of audiagnetotelluric soundings to determine the types of rocks and their geologic ages –A case study of the Eastern Edge of the Douala Sedimentary Basin in Cameroon. The 2nd International Conference on the Geology of Africa, Vol. (I), p-p. 787-797 Assuit, Egypt.
- [10]. **Dumort J. C. (1968).** Notice explicative sur la feuille de Douala – Ouest. Direction des Mines et de la Géologie du Cameroun, 69p, index, 1 carte h. t.

- [11]. **Morgan W. J.** (1972). Deep mantle convention plumes and plates motions. Am. Ass. Petrol. Geol. Bull. 56, 203-213
- [12]. **Deltheil J. R., Le Fournier J. and Micholet J., (1975).** Schema devolution sédimentaire d'une marge continentale stable: Exemple type du Golfe de Guinée, de l'Angola au Cameroun. IXème Congrès International de la sédimentologie. Mince-France.
- [13]. **Benderitter, Y. (1982).** Interprétation des mesures magnétotellurique obtenues avec un resistivimètre ECA, CNRS, CRG, Garchy.
- [14]. **Garcia, X., and Jones, A. G., (2001).** Atmospheric sources for audio-magnetotelluric (AMT) sounding. Geophysics, 67, 448-458.
- [15]. **Manguelle-Dicoum E., Nouayou R., Bokossah A. S. and Kwende-Mbanwi T. E. (1993).** Auomagnetotelluric soundings on the basement – sedimentary transition zone around the eastern margin of the Douala basin in Cameroon. Journal of African earth Sciences, Vol. 17, No. 4, pp. 487-497.
- [16]. **Groshong R. H. Jr (1999).** 3-D Structural Geology. A guide to structure and surface map interpretation. ISBN 3-540-65422-4 springer- Verlag Berlin Heidelberg Ne York.
- [17]. **Manguelle-Dicoum E. (1988).** Etude Géophysique des structures superficielles et profondes de la région de Mbalmayo. Thèse de Doctorat ès-sciences (Géophysique). Université de Yaoundé.
- [18]. **Njingti N., Manguelle-Dicoum E., Mbom-Abane, Tadjou J. M. (2001).** Evidence of major tectonic dislocations along the southern edge of the Pan African mobile zone and the Congo Craton contact in Southern region of Cameroon. The 2nd International Conference on the Geology of Africa, Vol. (I), p-p, 799-811 Assuit, Egypt.
- [19]. **Cagniard, L., (1953).** Principe de la méthode magnetotellurique, nouvelle méthode de prospection géophysique. Annales de Géophysique T. 9. 95-124.